This manuscript was accepted by J. Chem. Phys. Click here to see the version of record.

Water Dissociation on Ni(100), Ni(110) and Ni(111) surfaces: Reaction Path Approach to Mode Selectivity

H Seenivasan[1], Bret Jackson[2] and Ashwani K Tiwari[1, a)]

[1]*Department of Chemical Sciences, Indian Institute of Science Education and Research Kolkata, Mohanpur 741246, India*
[2]*Department of Chemistry, University of Massachusetts, Amherst, Massachusetts, 01003, USA*

ABSTRACT

A comparative study of mode-selectivity of water dissociation on Ni(100), Ni(110) and Ni(111) surfaces is performed at same level of theory using a fully quantum approach based on the reaction path Hamiltonian (RPH). Calculations show that the barrier to water dissociation on the Ni(110) surface is significantly lower compared to its close-packed counterparts. Transition states for this reaction on all three surfaces involve elongation of one of the O–H bonds. A significant decrease in the symmetric stretching and bending mode frequencies near the transition state is observed in all the three cases and in the vibrational adiabatic approximation, excitation of these softened modes results in significant enhancement in reactivity. Inclusion of non-adiabatic couplings between modes results in the asymmetric stretching mode showing similar enhancement of reactivity as symmetric stretching mode. Dissociation probabilities calculated at a surface temperature of 300K showed higher reactivity at lower collision energies compared to that of static surface case, underlining the importance of lattice motion in enhancing reactivity. Mode selective behavior is similar on all the surfaces. Molecules with one-quantum of vibrational excitation in the symmetric stretch, at lower energies (up to ~0.45 eV), are more reactive on Ni(110) than the Ni(100) and Ni(111) surfaces. However, the dissociation probabilities approach saturation on all the surfaces at higher incident energy values. Overall, Ni(110) is found to be highly reactive toward water dissociation among the low-index nickel

This manuscript was accepted by J. Chem. Phys. Click here to see the version of record.

surfaces owing to a low reaction barrier resulting from the openness and corrugation of the surface. These results show that mode-selective behavior does not vary with different crystal facets of Ni qualitatively, but there is a significant quantitative effect.

Corresponding author

[a)]Email: ashwani@iiserkol.ac.in

I. INTRODUCTION

Controlling the outcome of chemical reactions has been the longstanding goal of chemists. When most of the scientific community is marching towards this goal using different techniques, attention is drawn to the main question prominently investigated by the gas-phase and gas-surface dynamics communities: Which internal states best speed up a reaction? Early experiments in the field of laser excitation of molecules showed that in unimolecular and bimolecular gas-phase reactions, vibrational excitation of the reagents can lead to an enhancement in reactivity.[1,2] Both mode- and bond- selectivity is possible. In mode-selective reactions the enhancement in reactivity depends upon the nature of the vibration, and not simply the energy. Bond-selectivity occurs when a specific vibrational excitation leads to the preferential cleavage of a bond. With the availability of improved laser methodologies, mode- and bond- selective studies of many gas-phase and gas-surface reactions have become possible. These experiments have enabled the possible control of reactions at the level of individual quantum states, and brought into question the statistical behavior of many reactions. While excitation of one of the vibrational normal modes is necessary for studying mode-selectivity, mode selectivity is realized only under the condition that the intra-molecular vibrational energy redistribution (IVR) is slow compared to the reaction time scales. Within this context, owing to its industrial and fundamental importance and also due to the availability of well characterized

spectra, methane and its isotopolologues have been the playing ground for studying mode-selectivity and bond-specificity both in gas-phase as well as gas-surface reactions.[3–10] These experiments and theoretical studies were conducted using collisions of CH_4, CH_3D, CH_2D_2, and CHD_3 with Cl, O, H, and also with nickel and platinum surfaces. The following recent reviews give a detailed discussion of the theoretical and experimental aspects of mode and bond selective chemistry of CH_4 and H_2O in the gas phase as well as on surfaces.[7,10–15] It is to be noted that since the dynamics of gas-phase and gas-surface reactions involving the same molecule are similar in most cases, models used to explain gas-phase reactions are generally applicable to reactions at surfaces with necessary precautions.[16]

Similar to methane, gas-phase collision experiments of water molecules with halogens, oxygen, and also with metal surfaces offer interesting chemistry, and the reactions involving metal surfaces are important in the context of heterogeneous catalysis. Owing to this importance, there has been a surge in the number of investigations of the dynamical aspects of water dissociation on metal surfaces. Since copper based catalysts are used industrially, initial quantum dynamical studies concentrated on understanding water dissociation on Cu(111) surfaces.[17–20] These studies invariably suggested that the vibrational excitation of the water normal modes resulted in significant enhancement in reactivity for H_2O and HOD molecules on Cu(111) surfaces using high (6-D) and reduced (3-D) dimensional potential energy surfaces (PES). In addition, they also emphasized that rotational excitation increases reactivity, and the reaction probability also varies with the initial orientation of water molecule. Recently, in a combined experimental and theoretical study, it was shown that D_2O molecule, similar to methane dissociation exhibits mode selective behavior on Ni(111).[21] Using molecular beam experiments and a scaled 6-D PES they showed that the asymmetric stretching frequency has a larger efficacy

This manuscript was accepted by J. Chem. Phys. Click here to see the version of record.

for promoting reaction compared to an increase in translational energy. A semiquantitative agreement was found between the theoretical and experimental results. Very recently, a 9-dimensional PES for water dissociation on Ni(111) was constructed by Guo and coworkers[22] using permutation invariant polynomial neural networks (PIP-NN)[23,24]. In a series of studies, they examined the effects of impact sites, incident angles and electron-hole pair excitation on the reaction probability using quasi classical trajectories and quasi-7-D quantum dynamics. A surface site-averaging model using the 9-D PES was successful in reproducing experimental trends[25] while electron-hole pair excitations, included using the friction approach, did not significantly modify the dynamics.[26] More recently, it was argued that the theoretical results did not quantitatively reproduce the experiments due to the deficiency of the PW91 functional used to construct the PES.[27,28] Though usage of the RPBE functional increased the barrier to reaction, quantitative agreement was not achieved.[29] While an accurate 9-D PES should give reasonable results for water dissociative chemisorption on metal surfaces, assuming that the results can be corrected for the effects of lattice motion, constructing such a surface and performing quantum dynamics is computationally expensive. This has led to a search for alternate methods involving less computational effort while still capturing the physics underlying the problem. With quantum effects accurately included, semiclassical and quasiclassical descriptions of the dynamical events are promising.[30] As suggested in a recent review, approximate methods are required while the limitations posed by them are to be studied, understood and appreciated.[31] One such approach is based on the reaction path Hamiltonian (RPH) proposed by Miller *et al*. for polyatomic molecules.[32] Recently, Jackson and co-workers have used the quantum form of the RPH to study the dissociative chemisorption of CH_4 on Ni and Pt surfaces.[7,33] They were successful in explaining mode-selectivity and bond-specificity in methane and its isotopologues on various

nickel and platinum surfaces.[33–39] Very recently, they studied H_2O, HOD and D_2O dissociation dynamics on Ni(111) and were able to explain the D_2O/Ni(111) experiments with acceptable success by performing quantum dynamics using the coupled wavepacket method on the reaction path PES.[40] They also included lattice site averaging and surface lattice motion using sudden models developed earlier for methane dissociation on metal surfaces.[41–43] In a similar spirit, the mode-selectivity of CH_4 on Ni(111) was studied by Krishnamohan *et al* who computed the vibrationally adiabatic PESs.[44] Using Massey velocities and parameters, they estimated transition rates between these surfaces at the avoided crossings. Their results suggested that the excitation of symmetric stretching is three times more efficient at promoting reaction than the excitation of the asymmetric stretching mode.

The studies mentioned above have concentrated mainly on the close-packed {111} facets of nickel or copper surfaces. However, industrially employed catalysts expose several different facets to reacting molecules, necessitating a study of the differences in reactivity each facet has to offer. Studies revealing crystallographic specificity for the three low-indexed planes of few *fcc*-metal surfaces are available in literature. On bare Pt(100), Pt(110) and Pt(111) surfaces, measured mean square displacements of surface lattice atoms are largest for motion along the surface normal, and the values are found to be largest for the (110) facet.[45] This type of motion is known to strongly affect reactivity[33–43]. The stepped nature of the *fcc*(110) plane provides more variety in possible adsorption sites than is available on flat surfaces. In this sense, it is noted that the (110) plane is the most highly symmetrical of all possible *fcc* stepped surfaces.[46] In earlier studies of water on the (111), (100) and (110) surfaces of Ni, differences in behaviour were identified by Benndorf and Madey using electron stimulated desorption ion angular distributions (ESDIAD), thermal desorption spectroscopy (TDS) and low energy electron diffraction (LEED)

techniques.[47] However, these studies do not give any evidence of water dissociation on the (100) and (111) planes while dissociation takes place at higher temperatures on the (110) face of Ni.[47,48] The row-and-trough structure of Ni(110) provides sufficient corrugation for formation of strong H_2O-Ni bonds, and a weakening of O–H bonds in the adsorbed water molecule facilitates dissociation. DFT studies from our group also showed that Ni(110) is more reactive among the three low index nickel surfaces.[49,50] Recent DFT studies of the water gas shift reaction on Ni(111), Ni(110) and Ni(100) surfaces also observed a lower barrier for H_2O dissociation on Ni(110), consistent with our findings.[51]

Similar trends are observed with other adsorbates like H_2 and CH_4. DFT studies of H_2 dissociation, and sticking found that the reaction on Ni(111) is activated while it is direct on Ni(110)[52] where dissociation occurs over the top site more favorably on a rougher surface than on close packed surfaces. Studies of the dissociation dynamics of H_2 on Ni(111), Ni(100) and Ni(110) surfaces using many body expansion potentials and classical trajectory methods showed that Ni(110) is highly reactive compared to the close packed surface.[53] Again, higher reactivity is attributed to structurally rough surfaces showing strong electronic corrugation where huge variations in the potential along the crests and troughs of the surfaces are seen. A comparatively large amount of information on crystallographic specificity is available for methane dissociation on nickel and platinum surfaces. Alignment dependent chemisorption studies of vibrationally excited CH_4 on Ni(100), Ni(110) and Ni(111) showed that the alignment along the plane of C-H stretch gave highest reactivity while the alignment along the surface normal showed lowest reactivity. Moreover, the largest alignment contrast between the maximum and minimum reactivity was found for Ni(110).[54] On the reconstructed Pt(110)-(1×2) surface[43], the motion of both first and third layer atoms were shown to effect the dissociation of methane, and while the

This manuscript was accepted by J. Chem. Phys. Click here to see the version of record.

effect of this lattice motion was strong, it was not significantly larger than that for dissociation on smoother surfaces.[35] Experiment has shown that methane is more reactive on the Pt(110)-(1×2) surface than on Pt(111) and Pt(100) surfaces.[55] The polar angle dependence of reactivity for molecules incident parallel to the missing row yields state-resolved site specific reactivity information consistent with Pt(110)-(1×2) reactivity in which the top layer Pt atoms located near the ridge sites dominate the reaction. For CH_4 on Pt(110)-(1×2), the concerted role of stretch and bend excitation was also reported.[28] From these reports it is understood that the higher reactivity of Pt(110)-(1×2) is due to lower coordination number for the ridge atoms compared to terrace atoms on Pt(111). These studies clearly show the difference in reactivity of low index metal surfaces towards various molecules and emphasize that the open, corrugated surfaces are more reactive compared to the close packed ones. However, there are no dynamics studies comparing the reactivity of H_2O on different facets of any metal surfaces.

Earlier studies from our group uncovered the differences in reactivity across the low-index nickel surfaces towards water dissociation, using DFT.[49,50] In those studies, the reaction path was assumed to be an inverted parabola and only information from the transition state was used to calculate the semiclassical tunneling probabilities. The effect of lattice motion was included using a sudden model, and an increase in surface temperature was shown to significantly increase reactivity in all cases. Other studies have reported that similar to CH_4 on metal surfaces, H_2O on metal surfaces exhibits mode-selectivity and bond-specificity and the three vibrational modes exhibit similar efficacy towards promoting the reaction.[21,40] This study is aimed at comparing the reactivity of water on close packed Ni(100) and Ni(111) surfaces with that of Ni(110) surface using the RPH approach. Although the results for H_2O dissociation on Ni(111) were published earlier[40], they are included here to compare and contrast with that of the

other two surfaces at the same level of theory. Quantum dissociation probabilities are calculated using an *ab-initio* PES for molecules in the ground state or with a one-quantum pre-excitation of various vibrational normal modes. The effect of lattice motion is included using a sudden model, and impact site averaging is treated using a harmonic energy-shifting approximation. The differences and similarities in reactivity of these surfaces towards water dissociation are studied in detail. While close packed surfaces behave similarly in many cases, comparison with an open and ridged Ni(110) surface will also give some insights into water interactions with stepped surfaces, and improve our understanding of surface corrugation effects on mode selectivity.

The paper is organized as follows. Section II gives the details of the electronic structure calculations, methods to construct the reaction path potential and implement the wavepacket dynamics. We also briefly describe the inclusion of lattice motion using a sudden model and the harmonic energy-shifting approximation. Results are presented and discussed in Section III. The paper concludes with the important results and a discussion of possible future work in Section IV.

II. METHODS

All total-energy calculations have been performed using the DFT-based Vienna *ab initio* simulation package (VASP).[56–59] A plane wave basis set is used with an energy cutoff of 400 eV. Spin-polarization was included in all the calculations. Nonlocal exchange-correlation effects are treated using the Perdew–Burke–Ernzerhof (PBE) exchange-correlation functional within the generalized gradient approximation (GGA).[60,61] Fully nonlocal optimized projector augmented-wave (PAW) potentials are used to describe the interactions between the ionic cores and electrons.[62,63] A slab supercell with periodic boundary conditions is used to model the nickel

This manuscript was accepted by J. Chem. Phys. Click here to see the version of record.

surface. The substrate and its repeatable images are separated by a vacuum space of 13 Å to avoid interaction with the adjacent slabs. The Ni(100), Ni(110) and Ni(111) substrates consist of four layers with 2 × 2 unit cells, corresponding to four metal atoms per layer. An equilibrium lattice constant of 3.522 Å for Ni was found from bulk geometry optimization, and used to construct the initial slabs. All four layers of the slab were then allowed to fully relax. The Brillouin zone was sampled by an 6×6×1 Γ-centered grid of *k*-points. For the calculation of molecule-surface energies, calculations are considered converged when all forces are smaller than 0.01 eV/Å.

The Climbing image-nudged elastic band (CI-NEB) method is used to identify molecular geometries along the reaction path.[64] The distance between these points along the MEP is given by the reaction path coordinate *s*, where $(ds)^2 = \sum_{i=1}^{9} dx_i^2$, and the x_i are the mass-weighted Cartesian coordinates of the water molecule. By convention, $s = 0$ denotes the transition state while negative and positive values for *s* correspond to reactant and product states, respectively. A PES is constructed by first calculating the total energy V_0 at various points along the reaction path. Normal mode analysis by diagonalizing the force constant matrix was preformed to extract the normal modes Q_k and corresponding frequencies $\omega_k(s)$ at these points. The normal modes Q_k, with *s*, form a new set of coordinates, related to the x_i by,

$$x_i = a_i(s) + \sum_{k=1}^{8} L_{i,k}(s) Q_k \qquad (1)$$

where, $a_i(s)$ describes the configuration of the molecule at point *s* and the eigenvectors from the normal mode calculation are $L_{i,k}(s)$. The Hamiltonian in reaction path coordinates is written:

This manuscript was accepted by J. Chem. Phys. Click here to see the version of record.

$$H = \frac{1}{2}p_s^2 + V_0(s) + H_{vib} - \frac{1}{4}(b_{ss}p_s^2 + 2p_s b_{ss}p_s + p_s^2 b_{ss}) - \frac{1}{2}(p_s\pi_s + \pi_s p_s) \quad (2)$$

where,

$$H_{vib} = \sum_{k=1}^{8}\left[\frac{1}{2}P_k^2 + \frac{1}{2}\omega_k^2(s)Q_k^2\right] \quad (3)$$

where p_s and P_k are the momenta conjugate to s and Q_k respectively, and

$$b_{ss} = \sum_{k=1}^{8} Q_k B_{k,9}(s) \quad (4)$$

and

$$\pi_s = \sum_{k=1}^{8}\sum_{j=1}^{8} Q_k P_j B_{k,j}(s) \quad (5)$$

The vibrationally non-adiabatic couplings, $B_{k,j}(s)$, are defined:

$$B_{k,j}(s) = \sum_{i=1}^{8} \frac{dL_{i,k}}{ds} L_{i,j}(s) \quad (6)$$

The Hamiltonian (Eqn. 2) is expanded to first order in b_{ss} and π_s. Earlier studies showed that higher order terms in b_{ss} and π_s are not important.[36,65] Energy flow between all modes k and j through the couplings $B_{k,j}$ is described by the π_s operator and coupling of the vibrational modes with the reaction coordinate (curvature coupling) is given by the operator b_{ss} through $B_{k,9}$.

The close-coupled wave packet approach is used to describe the total molecular wave function, which is written as follows

$$\Psi(s;t) = \sum_n \chi_n(s;t)\Phi_n(\{Q_k\};s) \quad (7)$$

This manuscript was accepted by J. Chem. Phys. Click here to see the version of record.

where Φ_n are the eigenfunctions of H_{vib} , with eigenvalues given by

$$\sum_{k=1}^{8} \hbar\omega_k(s)\left(n_k + \frac{1}{2}\right) \tag{8}$$

The index *n* denotes vibrational state corresponding to the set of quantum numbers $\{n_k\}$. These vibrationally adiabatic eigenfunctions are products of 1D harmonic oscillator eigenfunctions which have a parametric dependence on *s*. Using the Hamiltonian, the coupled equations of motion for the wave packets, $\chi_n(s; t)$ are defined by

$$i\hbar\dot{\chi}_n(s;t) = \left[\frac{1}{2}p_s^2 + V_0(s) + \sum_{k=1}^{8} \hbar\omega_k(s)\left(n_k + \frac{1}{2}\right)\right]\chi_n(s;t) + \sum_{n'} F_{nn'}\chi_{n'}(s;t) \tag{9}$$

In this formulation, *n=0* corresponds to the vibrationally adiabatic ground state, while *n=k* corresponds to a state with one vibrational quantum excited. Moreover, two quanta excited states are also included. The effective or vibrationally adiabatic potential, V_{eff}, on which the wavepackets propagate, is given by

$$V_{eff,n}(s) = V_0(s) + \sum_{k=1}^{8} \hbar\omega_k(s)\left(n_k + \frac{1}{2}\right) \tag{10}$$

These potentials are thus the zero point energy (ZPE) corrected MEP, plus the energy of any vibrational excitation, which can change along the path. The operators $F_{nn'}$ contain b_{ss} and π_s which couple vibrationally adiabatic states differing by one and two quanta, respectively. The parametric dependence of Φ_n on *s* leads to derivative coupling terms that are responsible for curve crossing between the vibrationally adiabatic potentials at higher velocities and for larger coupling values.[33,66,67] The equations are given in detail elsewhere.[40]

This manuscript was accepted by J. Chem. Phys. Click here to see the version of record.

Only six of the nine modes having highest frequencies near the transition state (TS) are included in the vibrationally adiabatic basis set. The other two modes with very low frequency correspond to the azimuthal orientation of the reacting O–H bond and the PES varies weakly with this motion. Given the equations of motion, standard techniques were used to evolve the wavepackets in time.[33,34] At large values of s, the reactive flux is Fourier transformed to give the vibrationally state resolved and energy resolved reaction probabilities[68,69], which we denote the static surface reaction probability $P_0(E_i, \mathbf{n})$. The reaction occurs with the O atom more or less on the top site on Ni(100) and Ni(111), where the barrier is lowest, whereas on Ni(110) the oxygen atom at the transition state is located between two of the top layer atoms and one second layer atom. For our normal incidence conditions, the position of the molecule in the X and Y directions (parallel to the surface plane) changes little as it follows the minimum energy path in the entrance channel and up to the TS. The rotational motion is treated adiabatically as the low frequency modes describing rotational motion remain in the ground state and are not coupled with the other modes.

Studies of methane[41–43], nitrogen[70] and hydrogen[71–73], and lately water dissociation[21,40] on metal surfaces invariably showed that the effect of lattice motion is important. The importance of including lattice motion when modeling gas-surface reactions is emphasized in a recent perspective that examines the dissociative chemisorption of CH_4 , H_2O and CO_2 on smooth and rough metal surfaces.[74] In this study, a well-accepted sudden model is used to include the effect of surface temperature.[41,42] This approach involves the calculation of two linear parameters, α (mechanical coupling), and β (electronic coupling), defined by $\Delta E_{barrier} = -\beta \Delta Q$, and $\Delta Z_{barrier} = \alpha \Delta Q$, where, Q is the lattice degree of freedom. $\Delta E_{barrier}$, and $\Delta Z_{barrier}$ account for the change in barrier height, and relative collision velocity, respectively, with the change in

This manuscript was accepted by J. Chem. Phys. Click here to see the version of record.

the position of lattice atom from equilibrium position (Q = 0). These parameters are calculated at the TS using DFT. On Ni(100) and Ni(111), the TS is modified, to a good approximation, only by the motion of the atom over which water dissociates. Put another way, the force on this atom, with the molecule at the TS, is significant while that on the other lattice atoms are comparatively very small. On the other hand, H_2O on Ni(110) is more complicated, as motion of more than one lattice atom can modify the TS. A similar observation was previously reported for methane dissociation on the reconstructed Pt(110)-(1×2) surface, when compared to Pt(100) and Pt(111).[35] The electronic coupling parameter, β on Ni(100) and Ni(111) surfaces was calculated as 0.75 and 0.65 eV Å^{-1}, respectively whereas on Ni(110), β = 0.50 and -0.65 eV Å^{-1} for top and second layer atoms, respectively. Since, on Ni(110), the transition state is located on three atoms, the dissociation probabilities on Ni(110) is an average of the values calculated with the β corresponding to these three atoms. Positive values of β describe the puckering of the lattice atom outside the surface, when the lattice atoms are allowed to relax, and thus decrease in barrier, while the negative β values describe the motion of lattice atom into the bulk (when lattice atoms are relaxed) which results in an increase in barrier height. The dissociation probability calculated using this corrected potential is Boltzmann averaged over all possible values of Q for a substrate temperature T (300 K in this case) using the lattice distortion energy calculated by DFT. Dissociation probabilities thus obtained are further improved by including the mechanical coupling, α, by averaging over the lattice atom momentum P, as described earlier.[42] The mechanical coupling parameter, α, was calculated to be similar on Ni(100) and Ni(111) surfaces with values, α = 0.82 and 0.84 while on Ni(110), α = 0.42. The final dissociative sticking probability is calculated by averaging the reaction probabilities over the impact sites X and Y away from top sites using an energy-shifting approximation as given below:

This manuscript was accepted by J. Chem. Phys. Click here to see the version of record.

$$P_0(E_i, n_0; X_0, Y_0) \approx P_0(E_i - \Delta V_{XY}(X_0, Y_0), n_0; X_0 = Y_0 = 0) \quad (11)$$

where ΔV_{XY} is the increase in barrier height at some position (X_0, Y_0) with respect to the top site calculated using the prescription in an earlier study.[7] This method worked well for methane dissociative chemisorption on Ni and Pt surfaces,[33–36] while it was only qualitatively successful in calculating the impact site-averaged reaction probabilities for water dissociation on Ni surfaces.[38,40] Since this description of site-averaging by the harmonic energy-shifting approximation takes into account only the increase in energy barrier relative to top site, this approximation is not sufficiently accurate to describe all gas-surface reactions. Recent studies of water dissociation on Ni(111) [22,25,27] and Cu(111)[75] showed that the reactivity depends not only on the barrier height but also on other features of the PES. These studies showed that it was more accurate to implement the site-averaging model by treating a 'sufficient' number of impact sites individually and at a high level of theory, and then averaging. Here, we attempt a qualitative full dimensional comparative study of water dissociation on three low-indexed Ni surfaces using a simple yet physically meaningful reaction path approach. We feel that it is sufficient to use the harmonic energy-shifting approximation to account for impact site averaging effects, rather than using a quantitatively more accurate but computationally expensive model.

III. RESULTS AND DISCUSSION

A. Reaction path and normal mode analysis

Potential energy, V_0 as a function of reaction coordinate, s is plotted in Fig. 1 for H_2O on Ni(100), Ni(110) and Ni(111) using 31, 26 and 25 grid points along the reaction path, respectively. A shallow well of 0.25, 0.38 and 0.17 eV was observed for the physisorption of H_2O on Ni(100), Ni(110) and Ni(111) surfaces, respectively. However, it is to be noted that the PBE functional does not include van der Waals forces, and therefore these values may not be

This manuscript was accepted by J. Chem. Phys. Click here to see the version of record.

accurate. We find that adsorption of H_2O is stronger on Ni(110) than on Ni(100) and Ni(111) surfaces. Corrugation in morphology has facilitated stronger adsorption on this surface. Transition states (TS) for water dissociation on the close packed Ni(100) and Ni(111) surfaces are similar while the open and corrugated Ni(110) is different from the close packed ones. On Ni(100) and Ni(111), at the TS, the oxygen atom lies more or over the Ni atom, while on Ni(110) the oxygen atom lies in between two Ni atoms constituting the short bridge site, and the dissociating H atom lies in the middle of the four-fold hollow site interacting with the second layer Ni atom. On all the three surfaces, the TS involves elongation of one of the O–H bonds and the bond distances are found to be 1.54, 1.35 and 1.57 Å on Ni(100), Ni(110) and Ni(111), respectively suggesting that vibrational excitation might increase reaction probability.

Vibrational frequencies of different normal modes along the reaction path have been calculated and shown in Fig. 2 (left panel). For water molecule far above the surface, 3 modes *viz.,* asymmetric stretching (v_{as}), symmetric stretching (v_{ss}) and bending (v_b) are non zero. The frequencies of the asymmetric stretching mode remain nearly unchanged at the transition state and even beyond the barrier, while a significant decrease in the symmetric stretching and bending mode frequencies is observed near the transition state in all three cases. Other translational and rotational modes at the asymptote become frustrated translations and rotations on interaction with the surface and the frequencies of these modes do not change appreciably. However, since the concern here is only vibrational mode-selectivity, these low frequency normal modes are not important in this study. Softening of symmetric stretching and bending modes suggests that the excitation of these modes would lead to a significant enhancement in reaction probabilities. In the vibrationally adiabatic approximation, excitation of symmetric stretching mode should increase the reaction probability more than any other mode.

Vibrational ZPE corrected potentials and the potentials corresponding to one-quantum excitation of vibrational normal modes of water are plotted in Fig. 2 (right panel). Barrier heights (E_b) calculated with respect to the water molecule far away from the surface on Ni(100), Ni(110) and Ni(111) are 0.71, 0.24 and 0.76 eV, respectively while vibrational zero-point energy (ZPE) corrections reduced the barrier by ~0.12 eV to 0.59, 0.12 and 0.63 eV, respectively. These values agree well with our previous results[49] while it slightly differs from the results of Farjamnia *et al.*[40] and Hundt *et al.*[21] This difference is most likely due to the usage of a 2 × 2 supercell in contrast to the 3 × 3 supercell used in other studies. The barrier heights reported in this study are approximately 0.04 eV less on Ni(100) and Ni(111) than those reported in our previous studies.[49] This slight decrease is attributed to the presence of a wide barrier in the minimum energy paths. In earlier studies, CI-NEB with few images was used to locate one point at the barrier, while in this case, we believe, calculations with more images have converged to a better value for the energy barrier. The points along the reaction paths are spline fitted to obtain the points on the grid used for wavepacket dynamics.

B. Reaction probabilities

Static surface reaction probabilities for H_2O dissociation on Ni(100), Ni(110) and Ni(111) surfaces for the vibrationally adiabatic and full coupling cases are calculated and plotted in Fig. 3. In the vibrationally adiabatic limit, reaction probabilities for the ground vibrational state are the lowest. Among the one-quantum vibrationally excited modes, the symmetric stretching mode shows the largest enhancement in reaction probability compared to ground state, while only a slight increase was found for excitation of the asymmetric stretching mode. The bending mode excitation showed higher reactivity compared to asymmetric stretching, while it was less than that obtained with the symmetric stretching mode. There is a sudden fall in the

This manuscript was accepted by J. Chem. Phys. Click here to see the version of record.

reaction probabilities *vs.* incident energy, at energies just below the energy barrier, where tunneling is the only way the reaction could proceed. All of this behavior, in the vibrationally adiabatic limit, can be explained by the significant decrease in the effective barrier height for the vibrationally excited modes with respect to the ground state (Fig. 2 (right panel)). These observations can be correlated with the mode-softening behavior observed for the symmetric stretching and bending modes at the transition state. On the other hand, no appreciable mode-softening was observed for the asymmetric stretching mode. On all the surfaces, in the vibrationally adiabatic limit, reaction probabilities are in the order: $V_{eff}<V_{as}<V_b<V_{ss}$. However, the probabilities for symmetric stretching and bending mode excitation in case of Ni(110) are very close to each other owing to negative barrier with respect to the gas phase. Although the barrier height with respect to water in the gas-phase is negative, it is worth noting that the barrier height is positive with respect to the water in the physisorbed state.

Switching on the coupling between the modes, $B_{k,j,}$ and the curvature coupling, $B_{k,9,}$ and thereby removing vibrational adiabaticity, changed the behavior significantly. Coupling between the states became possible and the excess vibrational energy is transformed into motion along the reaction path allowing dissociation of H_2O molecule even at low incident energies. Reactivity at lower energies is significantly increased in all cases. Though excitation of v_{as} mode showed lowest reaction probabilities among the vibrationally excited states in the adiabatic conditions, this mode exhibits probabilities almost equal to that of the v_{ss} mode, when coupling is included. Large coupling values between the symmetric and asymmetric stretching modes allowed these modes to couple in the entrance channel and show similar probabilities for these stretching vibrational modes. The behavior of H_2O/Ni(110) is exactly similar to that found on close packed surfaces, except that exciting the bending and symmetric stretching modes leads to a negative

This manuscript was accepted by J. Chem. Phys. Click here to see the version of record.

barrier with respect to the gas phase, which was not observed on close packed surfaces. Such high reaction probabilities were not observed for any of the close packed surfaces. Such high probabilities can be attributed to low reaction barriers for water dissociation on Ni(110). It is interesting to note that this reaction goes barrierless with respect to gas-phase H_2O, (though there is a barrier of 0.137 eV with respect to H_2O in adsorbed state) on excitation of the symmetric stretching and bending modes. This plot reveals clearly the mode-selectivity in the case of water dissociation on low-index nickel surfaces within the vibrationally adiabatic approximation. Similar mode-selective behavior was reported earlier for H_2O/Cu(111)[17,76] and H_2O/Ni(111)[27,40] using both RPH and high dimensional quantum dynamics methods. Overall, the mode-softening behavior is qualitatively similar on Ni(100), Ni(110) and Ni(111) surfaces and mode-selectivity does not vary significantly between different low-index facets of nickel.

Final dissociative sticking probabilities calculated by site-averaging $P_0(E_i, \mathbf{n})$ and including surface temperature effects at 300 K (following the experiments[21]) using sudden models are plotted in Fig. 4. The inclusion of lattice motion enhanced the dissociation probabilities, especially at energies below the barrier while the site-averaging decreased the reaction probabilities at all energies, with a significant effect at higher energies. The individual effects of electronic coupling (β), mechanical coupling (α) and site-averaging are explained below. The electronic coupling parameter, β, increased the reaction probabilities at all energies compared to the static surface case. The increase at lower energies is particularly large, as lattice motion makes over-the-barrier pathways to reaction possible. However, inclusion of the recoil effects through the mechanical coupling parameter, α, further increased the dissociation probabilities at lower energies and decreasing the reaction probabilities at high incident energies. This reduction is attributed to the recoil effects of the metal atom due to higher incident energies

This manuscript was accepted by J. Chem. Phys. Click here to see the version of record.

of the incoming water molecule. Increase in surface temperature from 0K to 300K increased reaction probabilities on all three surfaces, while the effect is pronounced in the case of Ni(100) due to the larger electronic coupling (β) values. Both mechanical (α) and electronic (β) coupling parameters are of equal importance for water dissociation as opposed to methane wherein the effect of β coupling was shown to be prominent. Comparing the lattice motion effects for methane and water, it was also noted that the surface temperature effect appears to be weaker for water than it is for methane dissociation on metal surfaces.[74] Site-averaging, on the other hand, decreased the reaction probabilities at least by an order of magnitude in Ni(100) and Ni(111). A decrease by approximately 2 orders of magnitude was found on Ni(110) as the barrier height increases very rapidly when moving away from the transition state on this surface. While the site-averaging model seems reasonably qualitative on the close-packed Ni(100) and Ni(111) surfaces, on Ni(110), where the barrier is low and the reactivity drops from ~1 to ~10^{-2} when averaging over different sites, its accuracy is questionable. It is likely that this decrease in reactivity is too large, suggesting that the harmonic energy-shifting approximation does not accurately capture the variation in reactivity with impact site for an open surface like Ni(110). Nevertheless, these findings reiterate the need of including lattice motion and site-averaging effects in gas-surface reactions to compare the reactivity with the molecular beam experiments.

To understand the differences between the reactivity of the three low-index nickel surfaces, dissociation probabilities at 300 K for ground state and one-quantum excited states in the symmetric and asymmetric stretching, and bending vibrational modes are plotted in Fig.5. For the ground vibrational state (Fig. 5a), the reactivity on Ni(110) is clearly large at all incidence energies, rapidly approaching saturation at higher incident energies. On Ni(100) and Ni(111), the dissociation probabilities increase with incident energies in the studied energy

This manuscript was accepted by J. Chem. Phys. Click here to see the version of record.

range. The values gets closer to that calculated on Ni(110) at high incidence energies. A similar trend is observed for the one-quantum excitation of the bending vibrational mode (Fig. 5c). However, for the bending mode, the reactivity on Ni(110) saturates earlier (~0.25 eV) than for the ground vibrational state, and the reactivities of Ni(100) and Ni(111) surfaces show similar values at ~0.8 eV. The trend in reactivities for both ground vibrational and the one-quantum excited bending modes is Ni(110) > Ni(100) > Ni(111). Dissociation probabilities exhibited by one quantum excited symmetric and asymmetric stretching vibration modes are similar at all incidence energies. Although the values follow the Ni(110) > Ni(100) > Ni(111) trend at incident energies up to ~0.4 eV and ~0.5 eV for symmetric and asymmetric stretching states, respectively, the reactivity of Ni(110) falls below the values calculated on Ni(100) and Ni(111) for energies above that. This decrease in reactivity, we believe, is mainly due to the site-averaging model used. Given a model that more accurately captures the impact site effects, it is expected that the reactivity of the Ni(110) surface will be higher than that seen on the Ni(100) and Ni(111) surfaces, owing to lower energy barriers on this open, corrugated surface. More accurate models for including other impact sites may show a qualitatively different behavior in the case of Ni(110). The reactivity approaches saturation at very high incident energies i.e., well above the barriers to reaction on all the surfaces. Moreover, vibrational excitation by one-quantum reduces the huge gap between the reactivities of the three surfaces at low incident energies.

Comparing the reactivity plots reveals that for all vibrational states studied here, the reactivity of H_2O on the Ni(110) surface is very high compared to that calculated for close packed Ni(100) and Ni(111) surfaces at the low collision energies relevant to real reactor conditions. This is primarily due to the difference in the energy barrier to the reaction. Ni(110) surface showed a very low barrier compared to other close packed surfaces due to its low-

This manuscript was accepted by J. Chem. Phys. Click here to see the version of record.

coordination number and corrugated geometry of the surface. Comparing the mode- and bond-selective behavior of methane on Ni and Pt surfaces, Crim suggested that changing the identity of the surface (different metal) has a greater effect compared to changing the crystal facet.[10] Our results on different crystal facets of nickel are consistent with this observation. To the best of our knowledge this is the first study to report a comparison of reactivity of low-index nickel surfaces towards water dissociation using a quantum dynamics approach.

C. Sudden vector projection (SVP) model

To explain the non-statistical nature of mode-selectivity, Guo and coworkers proposed a model based on the coupling between a reactant mode and the reaction coordinate mode at the transition state, called the 'sudden vector projection' (SVP) model.[77,78] The magnitude of this coupling determines the ability of a particular vibration to promote reaction. This is approximately quantified by the projection of the reactant normal mode onto the reaction coordinate, at the transition state. This model is valid in the sudden limit where it assumes that the collision time is faster than the time required for internal vibrational redistribution (IVR). Given the simplicity, this model predicted mode-selectivity for various unimolecular[79], gas phase[77] and gas-surface[80] reactions well. The SVP values calculated for H_2O on Ni(100), Ni(110) and Ni(111) surfaces are shown in Table I. The symmetric and asymmetric stretching modes have similar SVP overlaps in contrast to the vibrationally adiabatic picture which predicts that excitation of only the symmetric stretching mode enhances reactivity. SVP overlaps for the bending modes are seen to be lower than for the stretching modes on these surfaces. In contrast, full quantum studies on a 6-D PES and RPH found similar efficacies for all the three normal vibrational modes for D_2O/Ni(111).[21,40] We find the same result here for the full coupling case. The vibrational efficacy values calculated using the scaled 6-D potential were ~1.6 while those

This manuscript was accepted by J. Chem. Phys. Click here to see the version of record.

calculated with the RPH are close to 1 for all these vibrational normal modes. Since the bending and rotational mode frequencies are very low at the transition state, the SVP model is not able to predict the efficacy of these modes in a reliable manner. The SVP model predicts that mode-selectivity for H_2O dissociation on all nickel low-indexed surfaces will be similar, consistent with our quantum dynamics studies. Therefore, it is concluded that the corrugation and openness of the Ni(110) surface is mainly responsible for reducing the barrier to dissociation and does not affect mode-selectivity of the reaction.

IV. CONCLUSIONS

Water dissociation on Ni(100) and Ni(111) surfaces was studied and compared with that on the Ni(110) surface, using a reaction path Hamiltonian approach. The minimum energy path for water dissociation on all three surfaces was calculated and a normal mode analysis was performed on all the points along the reaction path. This normal mode analysis showed that the symmetric stretching and bending mode frequencies decreased significantly near the transition state (and beyond), while no appreciable change was found in the frequencies of the asymmetric stretching modes. The decrease in vibrational frequencies of various normal modes along the reaction path follows a similar trend on all surfaces. Within the vibrationally adiabatic approximation, excitation of vibrational normal modes by one quantum reduced the energy barrier for the reaction resulting in higher reaction probabilities. Negative barriers with respect to gas-phase H_2O were observed upon exciting symmetric stretching and bending modes, for reaction on Ni(110). However, on all the surfaces, excitation of the symmetric stretch reduced the effective (vibrationally adiabatic) barrier significantly and led to considerable enhancement in the reaction probability. Excitation of the bending modes led to a moderate enhancement in reactivity while the asymmetric stretching mode only slightly enhanced the reactivity compared

to the ground state. Under the static surface approximation, owing to a very low barrier, dissociation probabilities on Ni(110) showed values close to one on excitation of the symmetric stretch and bend modes. Inclusion of non-adiabatic couplings significantly enhanced the reactivity of the asymmetric stretching mode on all the surfaces. Mode selective behavior of water dissociation was observed on nickel surfaces and again this is similar on all surfaces studied. Surface corrugation was found to have little effect on the mode-selective behavior. On all the three surfaces, full-dimensional dissociative sticking probabilities were calculated by including surface temperature effects and by averaging over impact sites. This modified the probabilities significantly and hence these effects should be included in gas-surface scattering calculations in order to compare with molecular beam experiments. Overall, the Ni(110) surface clearly shows a higher reactivity towards water dissociation compared to close-packed Ni(100) and Ni(111) surfaces. But, the following question remains elusive and needs further investigation – Is the reaction barrierless on Ni(110) when H_2O is vibrationally excited?

Owing to the openness of the Ni(110) surface, the interaction energies and thus the PES show complexities for H_2O on Ni(110). The RPH approach was used to compare reactivity on all three surfaces under a similar footing. However, from the previous studies of CH_4 on Ni(110) and Pt(110)(1×2), and this study, it is clear that open surfaces are complex and offer a variety of effects like alignment and site specific reactivity, to mention a few. These effects can only be captured by developing a full-dimensional PES with reasonable accuracy and more importantly, experiments need to be performed to verify the predictions. To have complete understanding of water dissociation on the Ni(110) surface, one needs to develop a full dimensional PES on which quantum dynamical calculations can be performed. It is also hoped that this study will stimulate experiments in this direction in the near future.

ACKNOWLEDGMENTS

H. Seenivasan sincerely acknowledges Council of Scientific and Industrial Research (CSIR), India for financial support under grant no.09/921(0075)/2013 EMR-I. A. K. Tiwari thanks the Science and Engineering Research Board (SERB), India for its funding under the grant EMR/2015/001337. B. Jackson gratefully acknowledges support from the Division of Chemical Sciences, Office of Basic Energy Sciences, Office of Energy Research, U. S. Department of Energy, under Grant # DE-FG02-87ER13744.

References

[1] F.F. Crim, Science **249**, 1387 (1990).

[2] F.F. Crim, Acc. Chem. Res. **32**, 877 (1999).

[3] R.D. Beck, P. Maroni, D.C. Papageorgopoulos, T.T. Dang, M.P. Schmid, and T.R. Rizzo, Science **302**, 98 (2003).

[4] R.R. Smith, D.R. Killelea, D.F. DelSesto, and A.L. Utz, Science **304**, 992 (2004).

[5] D.R. Killelea, V.L. Campbell, N.S. Shuman, and A.L. Utz, Science **319**, 790 (2008).

[6] L. Chen, H. Ueta, R. Bisson, and R.D. Beck, Faraday Discuss. **157**, 285 (2012).

[7] S. Nave, A.K. Tiwari, and B. Jackson, J. Phys. Chem. **118**, 9615 (2014).

[8] P.M. Hundt, H. Ueta, M.E. van Reijzen, B. Jiang, H. Guo, and R.D. Beck, J. Phys. Chem. **119**, 12442 (2015).

[9] F. Nattino, D. Migliorini, G.-J. Kroes, E. Dombrowski, E.A. High, D.R. Killelea, and A.L. Utz, J. Phys. Chem. Lett. **7**, 2402 (2016).

[10] F.F. Crim, Proc. Natl. Acad. Sci. **105**, 12654 (2008).

[11] L.B.F. Juurlink, D.R. Killelea, and A.L. Utz, Prog. Surf. Sci. **84**, 69 (2009).

[12] A.L. Utz, Curr. Opin. Solid State Mater. Sci. **13**, 4 (2009).

[13] R.D. Beck and A.L. Utz, in *Dyn. Gas-Surface Interactions: At. Underst. Scatt. Process. at Surfaces* (Springer Berlin Heidelberg, Berlin, Heidelberg, 2013), pp. 179–212.

[14] B. Jiang, M. Yang, D. Xie, and H. Guo, Chem. Soc. Rev. **45**, 3621 (2016).

[15] H. Chadwick and R.D. Beck, Chem. Soc. Rev. **45**, 3576 (2016).

[16] F.F. Crim, Faraday Discuss. **157**, 9 (2012).

[17] B. Jiang, X. Ren, D. Xie, and H. Guo, Proc. Natl. Acad. Sci. **109**, 10224 (2012).

[18] B. Jiang, D. Xie, and H. Guo, Chem. Sci. **4**, 503 (2012).

[19] B. Jiang, J. Li, D. Xie, and H. Guo, J. Chem. Phys. **138**, 044704 (2013).

[20] A. Mondal, H. Seenivasan, and A.K. Tiwari, J. Chem. Phys. **137**, 094708 (2012).

[21] P.M. Hundt, B. Jiang, M.E. van Reijzen, H. Guo, and R.D. Beck, Science **344**, 504 (2014).

[22] B. Jiang and H. Guo, Phys. Rev. Lett. **114**,166101 (2015).

[23] B. Jiang and H. Guo, J. Chem. Phys. **139**, 204103 (2013).

[24] B. Jiang and H. Guo, J. Chem. Phys. **141**, 034109 (2014).

[25] B. Jiang and H. Guo, J. Chem. Phys. **143**, 164705 (2015).

[26] B. Jiang, M. Alducin, and H. Guo, J. Phys. Chem. Lett. **7**, 327 (2016).

[27] B. Jiang, H. Song, M. Yang, and H. Guo, J. Chem. Phys. **144**, 164706 (2016).

[28] R. Bisson, M. Sacchi, and R.D. Beck, Phys. Rev. B **82**, 121404 (2010).

[29] B. Jiang and H. Guo, Phys. Chem. Chem. Phys. **18**, 21817 (2016).

[30] H. Guo, **131**, 1077 (2012).

[31] K. Golibrzuch, N. Bartels, D.J. Auerbach, and A.M. Wodtke, Annu. Rev. Phys. Chem. **66**, 399 (2015).

[32] W.H. Miller, N.C. Handy, and J.E. Adams, J. Chem. Phys. **72**, 99 (1980).

[33] B. Jackson and S. Nave, J. Chem. Phys. **135**, 114701 (2011).

[34] B. Jackson and S. Nave, J. Chem. Phys. **138**, 174705 (2013).

[35] D. Han, S. Nave, and B. Jackson, J. Phys. Chem. **117**, 8651 (2013).

[36] M. Mastromatteo and B. Jackson, J. Chem. Phys. **139**, 194701 (2013).

[37] H. Ueta, L. Chen, R.D. Beck, I. Colon-Diaz, and B. Jackson, Phys. Chem. Chem. Phys. **15**, 20526 (2013).

[38] H. Guo and B. Jackson, J. Phys. Chem. C **119**, 14769 (2015).

[39] F. Nattino, H. Ueta, H. Chadwick, M.E. van Reijzen, R.D. Beck, B. Jackson, M.C. van Hemert, and G.-J. Kroes, J. Phys. Chem. Lett. **5**, 1294 (2014).

[40] A. Farjamnia and B. Jackson, J. Chem. Phys. **142**, 234705 (2015).

[41] A.K. Tiwari, S. Nave, and B. Jackson, Phys. Rev. Lett. **103**, 253201 (2009).

[42] A.K. Tiwari, S. Nave, and B. Jackson, J. Chem. Phys. **132**, 134702 (2010).

[43] S. Nave, A.K. Tiwari, and B. Jackson, J. Chem. Phys. **132**, 054705 (2010).

[44] K.G. Prasanna, R.A. Olsen, A. Valdes, and G.-J. Kroes, Phys. Chem. Chem. Phys. **12**, 7654 (2010).

[45] H.B. Lyon and G.A. Somorjai, J. Chem. Phys. **44**, 3707 (1966).

[46] S.J. Jenkins and S.J. Pratt, Surf. Sci. Reports **62**, 373 (2007).

[47] C. Benndorf and T.E. Madey, Surf. Sci. **194**, 63 (1988).

[48] B.W. Callen, K. Griffiths, R.V. Kasza, M.B. Jensen, P.A. Thiel, and P.R. Norton, J. Chem. Phys. **97**, 3760 (1992).

[49] H. Seenivasan and A.K. Tiwari, J. Chem. Phys. **139**, 174707 (2013).

[50] H. Seenivasan and A.K. Tiwari, J. Chem. Phys. **140**, 174704 (2014).

[51] A. Mohsenzadeh, T. Richards, and K. Bolton, Surf. Sci. **644**, 53 (2016).

[52] G. Kresse, Phys. Rev. B **62**, 8295 (2000).

[53] C.-Y. Lee and A.E. DePristo, J. Chem. Phys. **84**, 485 (1986).

[54] B.L. Yoder, R. Bisson, P. Morten Hundt, and R.D. Beck, J. Chem. Phys. **135**, 224703 (2011).

[55] R. Bisson, M. Sacchi, and R.D. Beck, J. Chem. Phys. **132**, 094702 (2010).

[56] G. Kresse and J. Hafner, Phys. Rev. B **47**, 558 (1993).

[57] G. Kresse and J. Hafner, Phys. Rev. B **49**, 14251 (1994).

[58] G. Kresse and J. Furthmüller, Comput. Mater. Sci. **6**, 15 (1996).

[59] G. Kresse and J. Furthmüller, Phys. Rev. B **54**, 11169 (1996).

[60] J.P. Perdew, K. Burke, and M. Ernzerhof, Phys. Rev. Lett. **78**, 1396 (1997).

[61] J.P. Perdew, K. Burke, and M. Ernzerhof, Phys. Rev. Lett. **77**, 3865 (1996).

[62] P.E. Blöchl, Phys. Rev. B **50**, 17953 (1994).

[63] G. Kresse and D. Joubert, Phys. Rev. B **59**, 1758 (1999).

[64] G. Henkelman, B.P. Uberuaga, and H. Jonsson, J. Chem. Phys. **113**, 9901 (2000).

[65] B. Jackson, F. Nattino, and G.-J. Kroes, J. Chem. Phys. **141**, 054102 (2014).

[66] S. Nave and B. Jackson, Phys. Rev. B **81**, 233408 (2010).

[67] B. Jackson and S. Nave, J. Chem. Phys. **138**, 174705 (2013).

[68] D.H. Zhang, Q. Wu, and J.Z.H. Zhang, J. Chem. Phys. **102**, 124 (1995).

[69] J. Dai, John Z. H. Zhang, J. Phys. Chem. **100**, 6898 (1996).

[70] L. Martin-Gondre, M. Alducin, G.A. Bocan, R.D. Muiño, and J.I. Juaristi, Phys. Rev. Lett. **108**, 096101 (2012).

[71] M. Bonfanti, C. Díaz, M.F. Somers, and G.-J. Kroes, Phys. Chem. Chem. Phys. **13**, 4552 (2011).

[72] A. Marashdeh, S. Casolo, L. Sementa, H. Zacharias, and G.-J. Kroes, J. Phys. Chem. C **117**,

8851 (2013).

[73] A. Mondal, M. Wijzenbroek, M. Bonfanti, C. Díaz, and G.-J. Kroes, J. Phys. Chem. **117**, 8770 (2013).

[74] H. Guo, A. Farjamnia, and B. Jackson, J. Phys. Chem. Lett. **7**, 4576 (2016).

[75] Z. Zhang, T. Liu, B. Fu, X. Yang, and D.H. Zhang, Nat. Commun. **7**, 11953 (2016).

[76] T. Liu, Z. Zhang, J. Chen, B. Fu, and D. Zhang, Phys. Chem. Chem. Phys. **18**, 8537 (2016).

[77] B. Jiang and H. Guo, J. Chem. Phys. **138**, 234104 (2013).

[78] H. Guo and B. Jiang, Acc. Chem. Res. **47**, 3679 (2014).

[79] J. Li and H. Guo, J. Phys. Chem. **118**, 2419 (2014).

[80] B. Jiang, M. Yang, D. Xie, and H. Guo, Chem. Soc. Rev. **45**, 3621 (2016).

Tables

TABLE I. Vibrationally adiabatic barrier heights (E_b), and sudden vector projection (SVP) values for H_2O dissociative chemisorption in the ground state or with one quantum of vibrational excitation, on Ni(100), Ni(110) and Ni(111).

	Barrier heights (E_b) , eV			**SVP values**		
Vib. state	**Ni(100)**	**Ni(110)**	**Ni(111)**	**Ni(100)**	**Ni(110)**	**Ni(111)**
gs	0.71	0.24	0.76	-	-	-
ν_{as}	0.57	0.08	0.61	0.695	0.647	0.618
ν_{ss}	0.28	-0.23	0.30	0.653	0.669	0.657
ν_b	0.49	-0.01	0.53	0.203	0.317	0.252

Figures

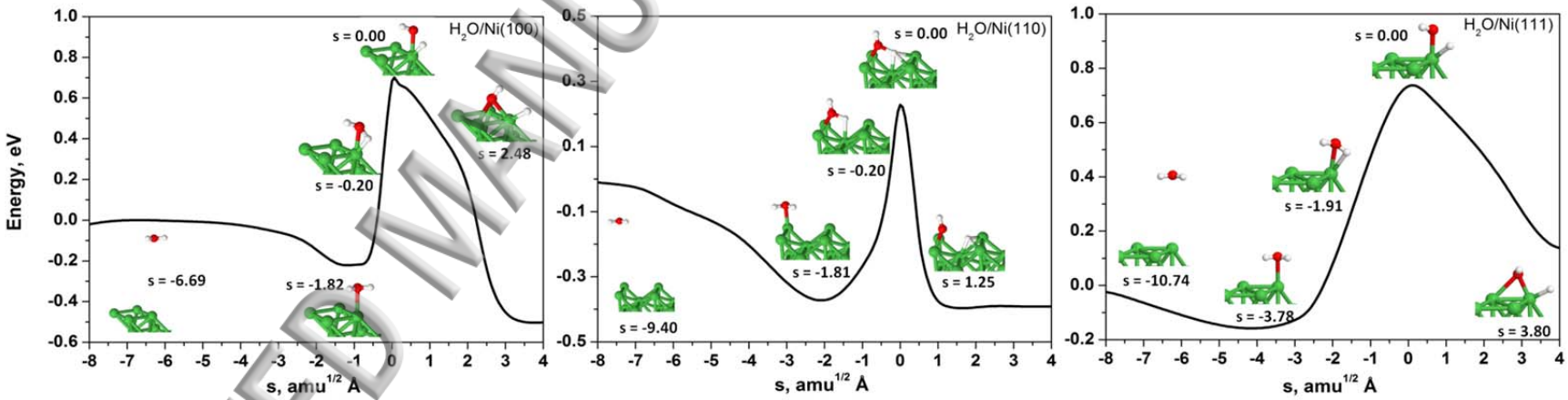

FIG. 1. As-calculated reaction path, $V_0(s)$, for H_2O dissociation on Ni(100), Ni(110) and Ni(111) surfaces calculated from DFT.

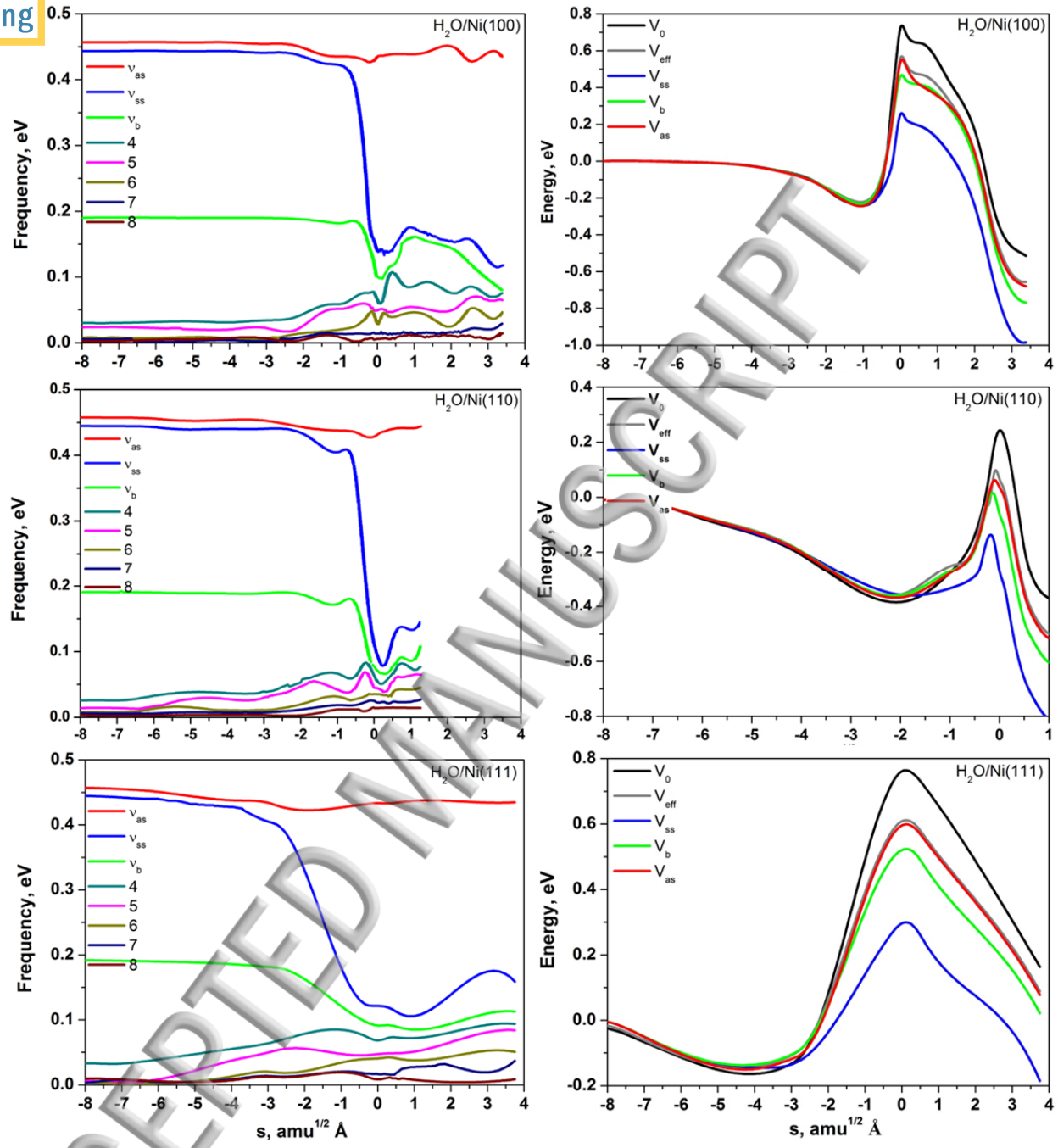

FIG. 2. Frequencies of various normal modes of H_2O along the reaction path; for water dissociation on Ni(100), Ni(110) and Ni(111). V_{as} corresponds to asymmetric stretching, V_{ss} to symmetric stretching and V_b to bend modes. Other numbered modes (4-8) correspond to frustrated translational and rotational modes (Left panel). Vibrational zero-point energy (ZPE) corrected potentials and the potentials corresponding to one-quantum excitation in various vibrational modes of H_2O. V_{eff} corresponds to the ZPE corrected ground state potential and V_{as} to asymmetric stretching, V_{ss} to symmetric stretching and V_b to bend modes (Right panel).

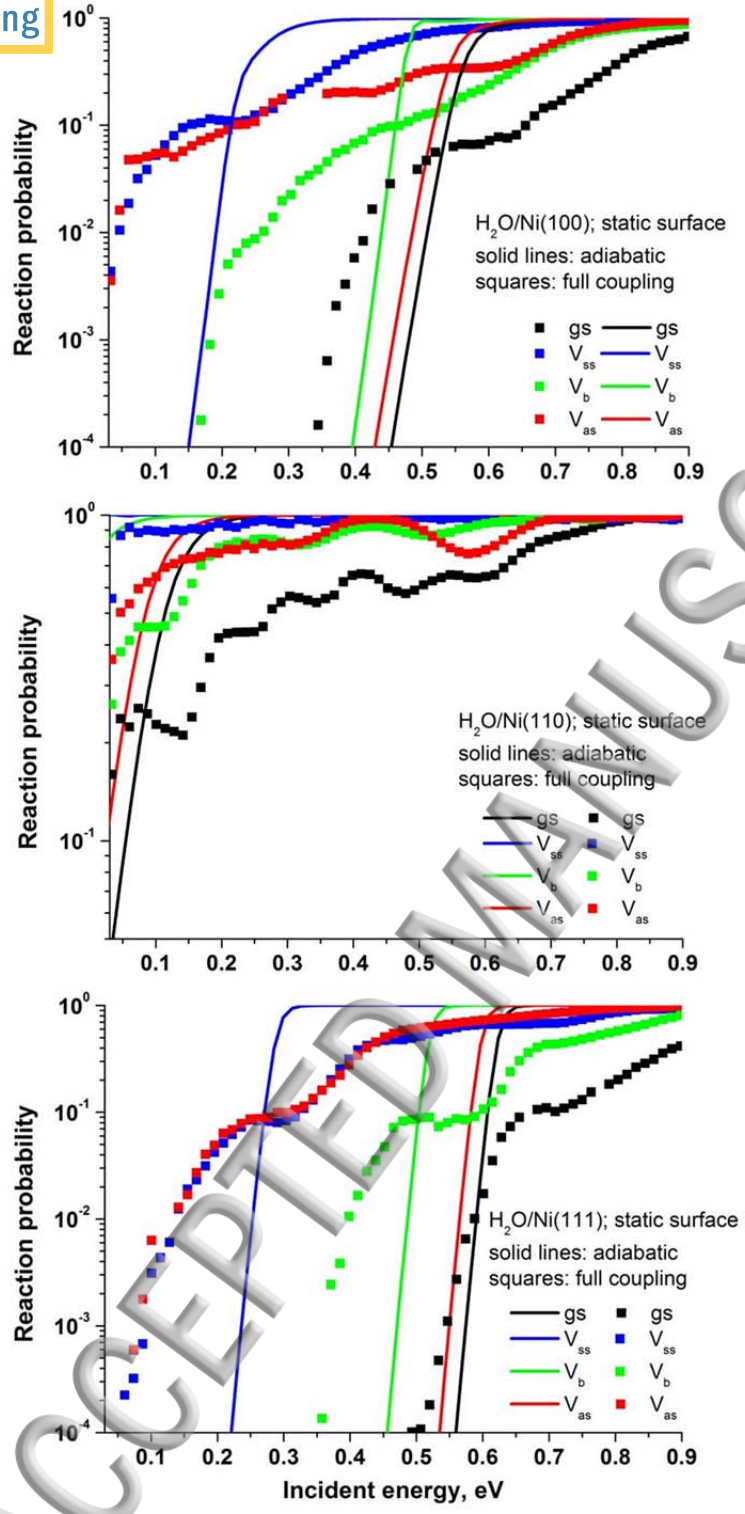

FIG. 3. Reaction probabilities as a function of incident energies for H_2O in vibrational ground state (gs) and several initial vibrationally excited states as mentioned in the figure, for H_2O dissociation on Ni(100), Ni(110) and Ni(111) surfaces under the static surface approximation.

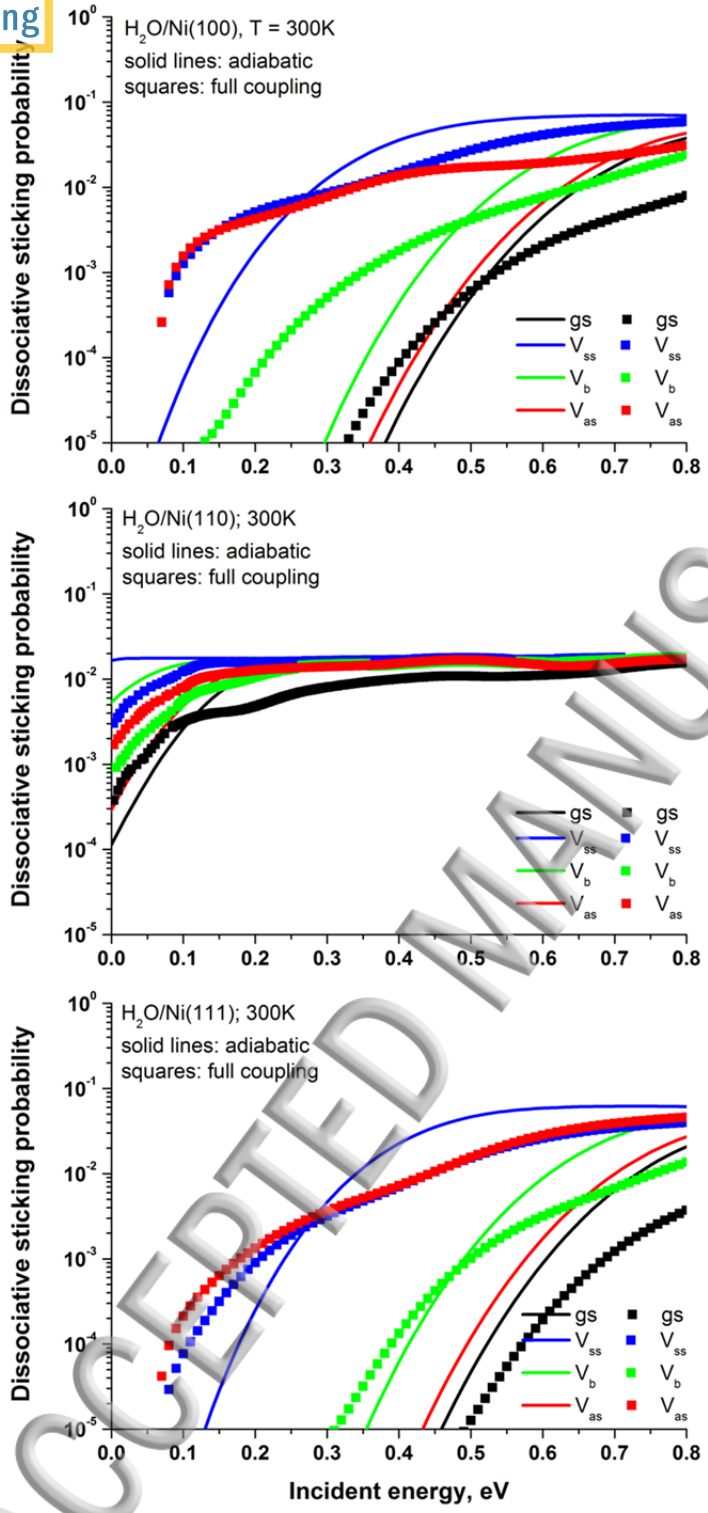

FIG. 4 Dissociation sticking probabilities as a function of incident energies for vibrational ground state and several initial vibrationally excited states of H_2O on Ni(100), Ni(110) and Ni(111) surfaces at 300 K.

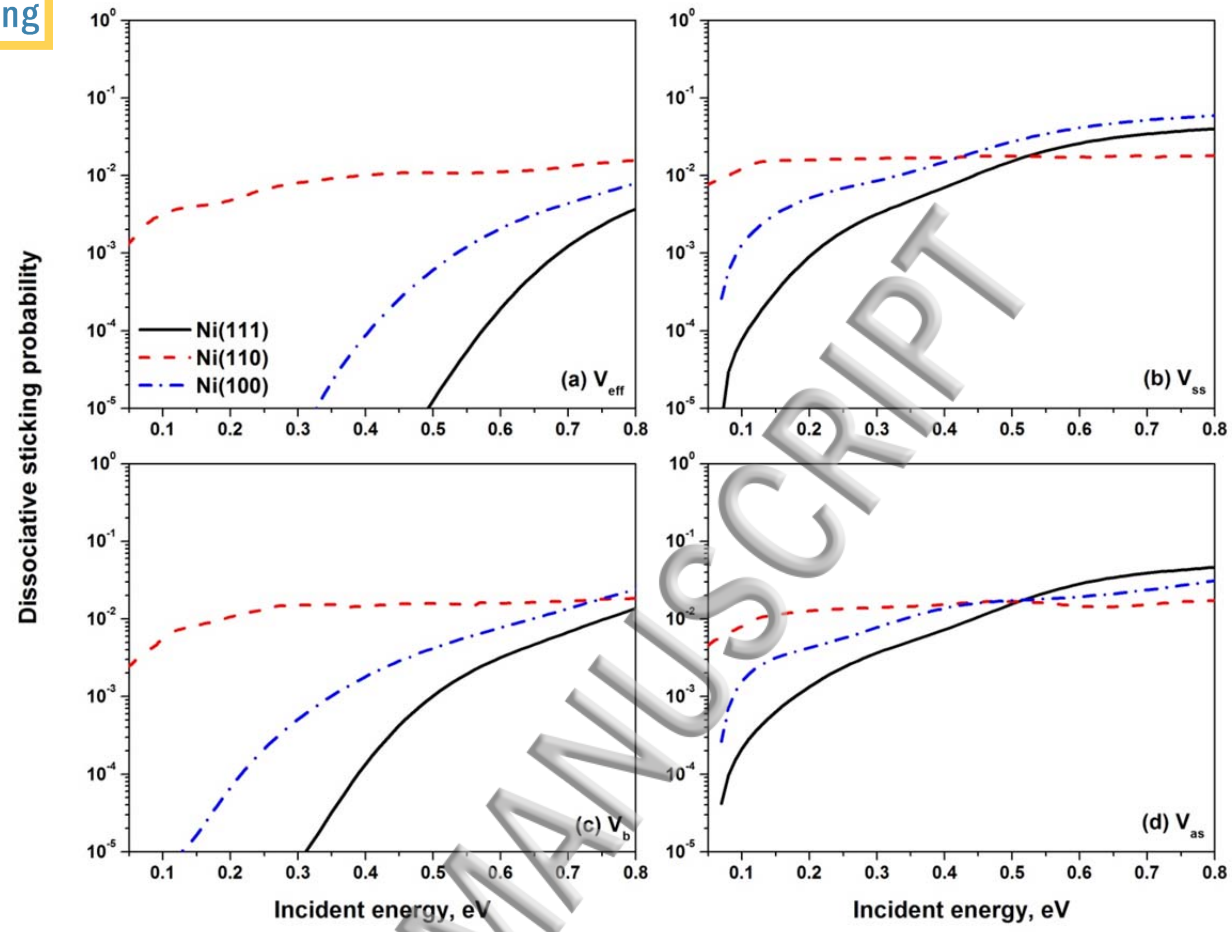

Fig. 5. Comparison of vibrational ground state reactivity and reactivity of normal modes excited by one-quantum for H_2O dissociation on Ni(100), Ni(110) and Ni(111) calculated at 300K.

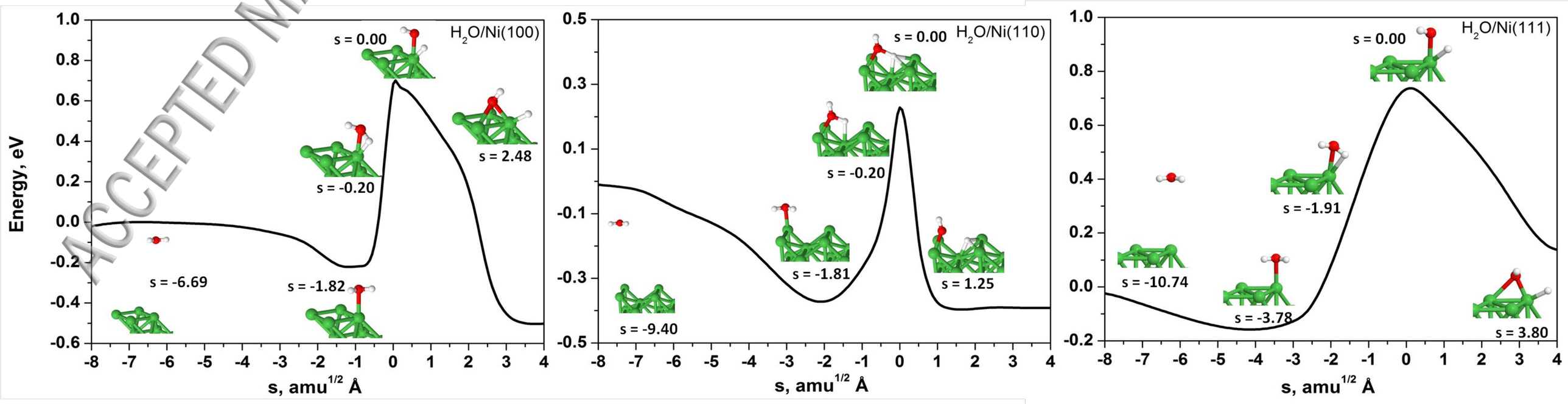
H2O/Ni(100)
s = 0.00
s = -0.20
s = 2.48
s = -6.69
s = -1.82
Energy, eV
s, amu1/2 Å
H2O/Ni(110)
s = 0.00
s = -0.20
s = -1.81
s = 1.25
s = -9.40
s, amu1/2 Å
H2O/Ni(111)
s = 0.00
s = -1.91
s = -10.74
s = -3.78
s = 3.80
s, amu1/2 Å